AGU PUBLICATIONS

JGR

Journal of Geophysical Research: Space Physics

RESEARCH ARTICLE
10.1002/2016JA022873

Key Points:
- EPBs occurrences show equinoctial maximum throughout 2001-2012 except for solar minimum 2007-2009
- Impact of solar activity on EPBs shows seasonal effects with the maximum during equinox season
- The 24 November magnetic storm triggers the EPB occurrence, whereas 6 November suppresses the EPB occurrence

Correspondence to:
S. Kumar,
sanjay.skitvns@gmail.com

Citation:
Kumar, S., W. Chen, Z. Liu, and S. Ji (2016), Effects of solar and geomagnetic activity on the occurrence of equatorial plasma bubbles over Hong Kong, *J. Geophys. Res. Space Physics*, *121*, 9164–9178, doi:10.1002/2016JA022873.

Received 28 APR 2016
Accepted 1 SEP 2016
Accepted article online 4 SEP 2016
Published online 22 SEP 2016

Effects of solar and geomagnetic activity on the occurrence of equatorial plasma bubbles over Hong Kong

Sanjay Kumar[1,2], Wu Chen[1], Zhizhao Liu[1], and Shengyue Ji[3]

[1]Department of Land Surveying and Geo-Informatics, Hong Kong Polytechnic University, Hong Kong, [2]Banaras Hindu University, Varanasi, India, [3]China University of Petroleum (Huadong), Qingdao, China

Abstract In the present study, the occurrence and characteristics of equatorial plasma bubble (EPB) has been analyzed using the GPS data from continuously operating reference stations network over Hong Kong during 2001–2012. The analysis found maximum EPB occurrences during the equinoctial months and minimum EPB occurrences during the December solstice throughout 2001–2012 except during the solar minimum in 2007–2009. The maximum EPB occurrences were observed in June solstice during 2007–2008, whereas for 2009, EPB occurrences were quite higher for June solstice but slightly smaller than the March equinox. The seasonal maximum in EPB occurrences have been discussed in terms of plasma density seed perturbation caused by gravity waves as well as the post sunset F-layer rise due to the pre-reversal enhancement of zonal electric field. Generally, EPB occurrences are found to be more prominent during nighttime hours (19:00–24:00 h) than daytime hours. The day and nighttime EPB occurrences were inferred and found to vary linearly with solar activity and have an annual correlation coefficient (R) of ~ 0.92 with $F_{10.7}$ cm solar flux and ~0.88 with sunspot number. Moreover, the impact of solar activity on EPB occurrences is found to be dependent on seasons with maximum during the equinox ($R = 0.80$) and minimum during the summer season ($R = 0.68$). The detail study of EPB occurrences during two typical cases of geomagnetic storms on 6 November and 24 November 2001 found that the storm on 24 November triggered the EPB occurrence whereas storm on 6 November suppressed the EPB occurrence. The enhancement/suppression of EPB occurrences during storms periods is a consequence of a storm-induced prompt penetration electric field as well as disturbance dynamo electric field effects associated with the main phase of the geomagnetic storm.

1. Introduction

The equatorial plasma bubbles (EPBs) are associated with the depletion in the plasma density, and they are observed most frequently in the pre-midnight sector [*Woodman and LaHoz*, 1976]. The presence of EPBs is due to the fast recombination of postsunset in the *E* region ionosphere that can produce an abrupt vertical plasma density gradient toward the *F* region of ionosphere. The plasma density gradient combines with the prereversal enhancement (PRE) of the zonal electric field, drives vertical $E \times B$ plasma drift. The plasma drift further causes plasma instability on the bottomside of the *F* region by the well-known generalized Rayleigh-Taylor (R-T) instability mechanism [*Fejer et al.*, 1999; *Basu et al.*, 2002; *Heelis*, 2004; *Kelley*, 2009]. The formation of EPBs is expected to cause interruption to the radio wave communication/navigation system by producing fluctuation in amplitude and phase of the radio signal known as scintillations [*Chen et al.*, 2008]. Therefore, forecasting of EPBs has been the topic of major research and has drawn the attention of the scientific community in the past years [e.g., *Tsunoda*, 1985; *Aarons*, 1993; *Huang et al.*, 2002; *Burke et al.*, 2004a, 2004b; *Nishioka et al.*, 2008; *Sripathi et al.*, 2011].

EPB occurrences have temporal (daily and seasonal) and longitudinal dependence [*Huang et al.*, 2002; *Makela et al.*, 2004]. The magnitude of the longitudinal gradient in the *E* region conductivity plays a significant role in seasonal occurrences of EPB. The alignment of the day-night terminator with the magnetic field is responsible for the occurrences of maximum EPBs [*Tsunoda*, 1985]. Using global observations, this theory has been supported by previous works [*Aarons*, 1993; *Huang et al.*, 2001, 2002; *Burke et al.*, 2004b; *Nishioka et al.*, 2008; *Su et al.*, 2008]. The other parameters controlling the EPB occurrences are the solar and geomagnetic activities. It has been shown that the EPB occurrences vary with solar activity and are more prominent during high solar activity years [*Basu et al.*, 1988, 2002; *Abdu et al.*, 1998]. Apart from the solar activity, the effect of magnetic storm on ionospheric plasma bubbles has also attracted a lot of attention over the past decade [e.g., *Aarons*, 1991; *Li et al.*, 2009; *Carter et al.*, 2014]. However, the occurrence of EPBs during magnetic storms has not been fully understood and its impacts on the occurrences of EPBs are found to be local time dependent of storm occurrence which can trigger or suppress the EPB occurrences [*Singh et al.*, 1997; *Huang*, 2011].

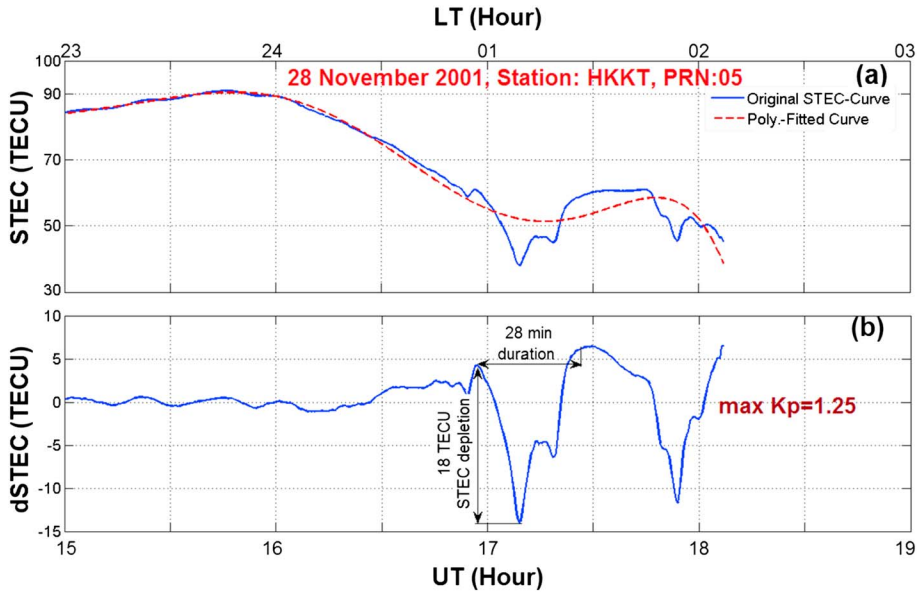

Figure 1. Time series of original STEC and best polynomial fitted curve observed by PRN 04 at HKST station, Hong Kong, during quiet day on (a) 28 November 2001; (b) the time series of detrended of STEC (dSTEC) showing characteristics of the plasma bubble.

In the past years several techniques such as ionosonde [*Rastogi*, 1980; *Abdu*, 2001], topside sounder [*Maruyama and Matuura*, 1984], radio scintillation [*Basu and Basu*, 1985; *Aarons*, 1993; *Iyer et al*., 2006], air glow observation [*Mendillo and Baumgardner*, 1982; *Patil et al*., 2016], and satellite-based measurements [*Huang*, 2011; *Huang et al*., 2014] have been used to study the characteristics of the plasma bubble. Due to difference in the signal wavelength used in different techniques, it is important to note that different kind of techniques are sensitive to plasma bubbles of different scale sizes [*kintner et al*., 2004; *Iyer et al*., 2006]. Therefore, each technique has its own advantage in the study of plasma bubble (ionospheric irregularities) of different scale sizes. In the recent years, GNSS (Global Navigation Satellite System) have become an important tool for ionospheric plasma bubble study [*Nishioka et al*., 2008; *Ji et al*., 2011] because of its growing application in civilian and military applications. Using ground-based GPS measurements over different regions, the seasonal occurrence of the plasma bubbles has been studied by the several workers [*Basu et al*., 1988; *Makela et al*., 2004; *Rama Rao et al*., 2006a, 2006b; *Portillo et al*., 2008; *Yokoyama et al*., 2011; *Sripathi et al*., 2011; *Liu et al*., 2015], but none of these studies using GPS have been done for a complete solar cycle.

In this study the data observed over 12 ground-based GPS stations in Hong Kong region, during more than a solar cycle from 2001 to 2012, have been used to study the occurrences of EPB. The effect of solar and geomagnetic activity on EPB occurrences has also been studied. Since our study period from 2001 to 2012 covers a period of solar minimum and solar maximum therefore, effort has also been made to distinguish the seasonal occurrence of EPB during solar minimum with those from the solar maximum.

2. Data and Method

The GPS data recorded over the Hong Kong from continuously operating reference stations (CORS) network have been analyzed. This network called Hong Kong satellite positioning reference station network (SatRef), consisted of six continuously operating reference stations (CORS) when it was established in 2001. This network was expanded to 12 GPS stations in 2004 (Figure 1a) [*Ji et al*., 2013]. The geographic and geomagnetic coordinates of these GPS stations along with data availability period are listed in Table 1. In this study, the slant total electron content (STEC) is computed from dual-frequency GPS observation data with time resolution of 30 s and is further converted to the vertical TEC (VTEC) [*Langley et al*., 2002; *Kumar and Singh*, 2009].The rate of change of TEC index (ROTI) is normally used to observe the ionospheric perturbation or irregularities and can be defined as the standard deviation of rate of change of TEC (ROT) [*Pi et al*., 1997]. The ROTI over 5 min interval is computed from ROT of GPS-TEC data using the following equation:

Table 1. List of GPS Stations in Hong Kong With Their Geographic and Geomagnetic Coordinates Along With Period of Data Availability

Station Code	Station Name	Geographic Latitude	Geographic Longitude	Geomagnetic Latitude	Period of Data Availability
HKKT	KAM TIN	22°, 26′N	114°, 03′E	12°, 40′N	2001–2012
HKFN	PIK FUNG ROAD	22°, 29′N	114°, 08′E	12°, 43′N	2001–2012
HKLT	LAM TEI	22°, 25′N	113°, 59′E	12°, 39′N	2001–2012
HKMW	MUI WO	22°, 15′N	114°, 00′E	12°, 29′N	2004–2012
HKNP	NGONG PING	22°, 14′N	113°, 53′E	12°, 28′N	2004–2012
HKOH	OBELISK HILL	22°, 14′N	114°, 13′E	12°, 29′N	2004–2012
HKPC(former HKKY)	PENG CHAU	22°, 17′N	114°, 02′E	12°, 31′N	2001–2012
HKSC	STNECUTTERS	22°, 19′N	114°, 08′E	12°, 33′N	2004–2012
HKSL	SIU LANG SHUI	22°, 22′N	113°, 55′E	12°, 54′N	2001–2012
HKSS	SHAP SZE HEUNG	22°, 25′N	114°, 16′E	12°, 41′N	2004–2012
HKST	SHA TIN	22°, 23′N	114°, 18′E	12°, 38′N	2001–2012
HKWS	WONG SHEK	22°, 26′N	114°, 20′E	12°, 40′N	2004–2012

$$\mathrm{ROTI} = \sqrt{\langle \mathrm{ROT}^2 \rangle - \langle \mathrm{ROT} \rangle^2}$$

where ROT at epoch time t_k has been computed from TEC data having temporal resolution of 0.5 min (30 s), using the following equation:

$$\mathrm{ROT}(t_k) = \frac{\mathrm{TEC}(t_k) - \mathrm{TEC}(t_{k-1})}{t_k - t_{k-1}}$$

Generally, ROT is expressed in TEC unit (TECU)/min, 1 TECU = 10^{16} el/m^2.

An equatorial plasma bubble can generally cause a sudden change of the slant or vertical TEC value, which is followed by a recovery when the satellite-to-receiver ray path no longer passes through the bubble. Thus, a bubble can be detected in GPS-STEC data using the method proposed by *Portillo et al*. [2008]. In this method a best polynomial fit (sixth degree) to GPS-STEC for a chosen PRN (Pseudo Random Number) is made (see Figure 1a) with a window size of 15 min. The values produced by subtracting the best polynomial fitted to the STEC curve from the original STEC curve gives the detrended STEC (dSTEC) (Figure1b). The difference between the maximum and minimum values is the depletion depth of the plasma bubble and can be used as indicator for the occurrence of bubbles. The STEC depletions observed from a satellite with magnitude greater than 5 TECU and apparent duration between 10 min and 180 min are considered to be a plasma bubble [*Portillo et al*., 2008]. In this study, this method has been used to identify EPB occurrences over Hong Kong during 2001–2012. Figure 1 shows a typical case of plasma bubbles observed by satellite PRN 05 over Hong Kong GPS station HKKT on 28 November 2001 (quiet day with $Kp < 4$). It is clearly seen that two plasma bubbles observed by PRN 05 had durations of 28 min and 35 min and STEC depletion (or depth) of 17.91 TECU and 18.17 TECU, respectively. To study the monthly, seasonal and annual occurrences of EPB, only geomagnetic quiet days ($Kp \leq 4$) with elevation cut off 20° from 2001 to 2012 are considered for the analysis.

The monthly EPB occurrence for a particular year is computed using the following formula

$$\text{Monthly EPB occurrence}(\%) = \frac{\text{Number of EPBs observed during a month}}{\text{Total number of EPBs observed during a year}} \times 100$$

To study the seasonal EPB occurrence, a year has been grouped into four seasons, namely, March equinox (February to April), June solstice (May to July), September equinox (August to October), and December solstice (November to January) and seasonal EPB occurrence for a particular year is computed using the following formula

$$\text{Seasonal EPB occurrence}(\%) = \frac{\text{Number of EPBs observed during a season}}{\text{Total number of EPBs observed during a year}} \times 100$$

3. Results and Discussion

3.1. Monthly and Seasonal Occurrence of EPB

The analysis of monthly EPB occurrences during each year from 2001 to 2012 has been carried out which is shown in Figure 2. The observed plasma bubbles occurrence found maximum during the solar maximum year

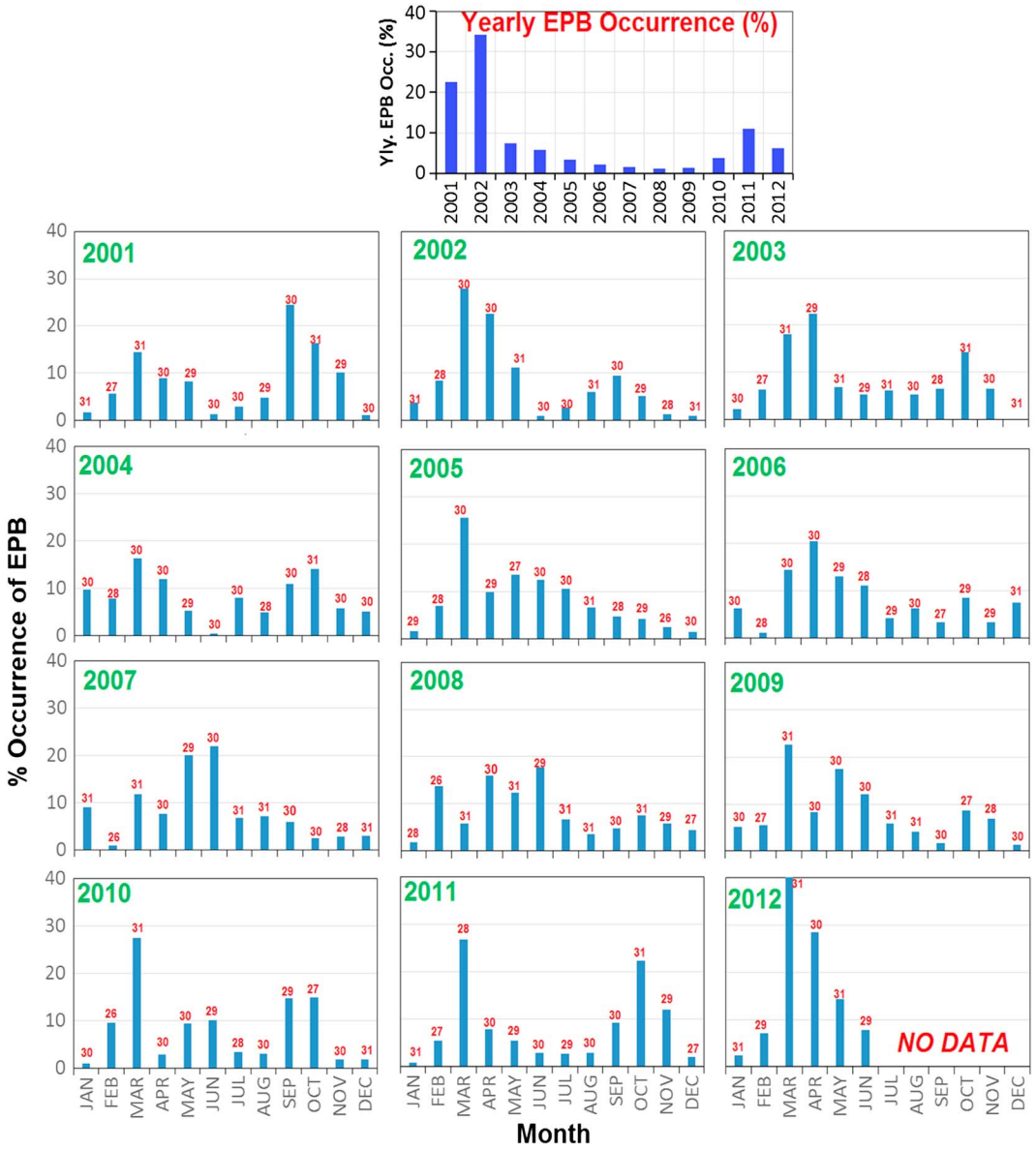

Figure 2. Monthly EPB Occurrences (%) from 2001–2011 and half year for 2012. The monthly percent EPBs for a year are computed with respect to total number of plasma bubbles observed during respective year. At the top most the yearly EPB occurrences (%) are also shown. The number written by red color above each bar represents the number of days on which GPS data are available in respective month.

of 2002. Monthly EPB occurrences show an equinoctial maximum throughout the year 2001–2012 except during the solar minimum years 2007–2008. During the years 2007–2008, maximum EPB occurrences were observed during June. Moreover, for the year 2009, the EPB occurrences during May and June were also found to be significantly larger than in September and October but smaller than March. To study the seasonal EPB occurrence, seasonal EPB occurrences for each year during 2001–2011 are shown in Figure 3. As evident from the monthly EPB occurrences, the seasonal EPB occurrences also show an equinoctial maximum throughout 2001–2012, except during the solar minimum in 2007–2009. The frequent equinoctial occurrences of plasma bubbles during the solar maximum year is due to fact that EPB attains a high altitude of around 800 km and above [*DasGupta et al.*, 1981; *Chakraborty et al.*, 1999].The seasonal and solar activity dependence of plasma bubble occurrences over the Hong Kong region is also found to be in agreement with EPBs reported using in situ measurements (ROCSAT-1 and DMSP) in the Southeast Asian region, i.e., the maximum occurrence probability of EPBs during equinoctial months in solar maximum years [e.g., *Burke et al.*, 2004a; *Su et al.*, 2008].

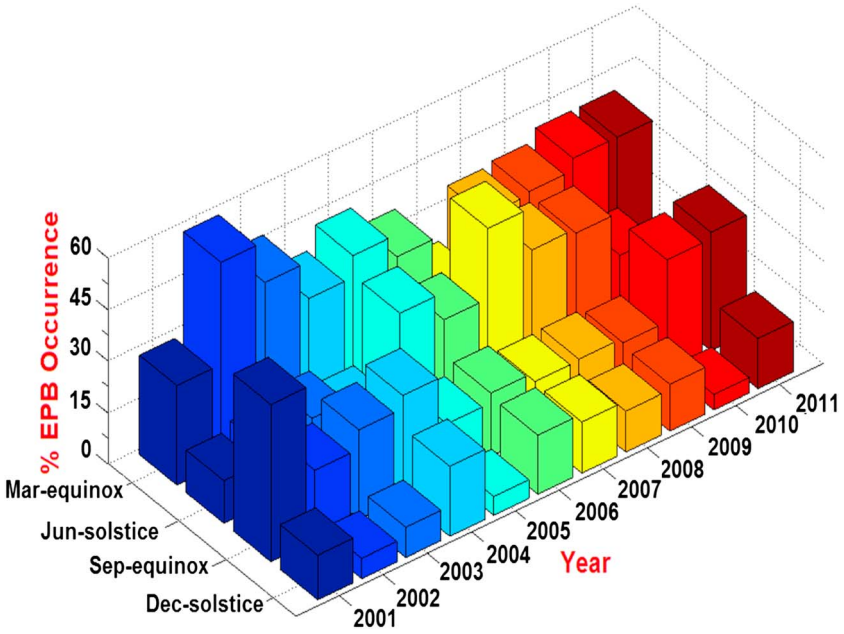

Figure 3. Percentage of EPB seasonal occurrences during 2001–2011. The observed plasma bubble occurrences showed equinoctial maxima throughout the year 2001–2011 except during the solar minimum years 2007–2009. It also showed the equinoctial asymmetry throughout 2001–2011, i.e., EPB occurrence rate at one equinox is higher than the other one.

The seasonal occurrence of EPB and severe scintillation activity is controlled by the magnetic declination angle (or angle between magnetic meridian and solar terminator). The alignment of the solar terminator with the magnetic meridian in two hemispheres plays an important role in producing maximum EPB occurrences during the equinox season [*Tsunoda*, 1985]. In equinox seasons, the alignment between the solar terminator and magnetic meridian becomes closer, which causes the reduction in the *E* region conductivity. It is important to notice that the *E* region is magnetically conjugate to the *F* layer, through which currents flow along the geomagnetic field lines. This flow of current connects the *F* region to the *E* regions on either side of the equator acting as a short circuit particularly in the sunlit hemisphere. The reduction of *E* region conductivity due to the alignment of the solar terminator with magnetic meridian is responsible for producing the $E \times B$ plasma drift in the equatorial *F* layer. This plasma drift creates a favorable situation for the formation of plasma bubbles during the equinox season. In addition, in the regions of westward/eastward longitude, the angle between the magnetic meridian and solar terminator minimizes EPB occurrences near to the June/December solstice [*Burke et al*., 2004a].

The interesting result of this study is that the plasma bubbles occurrences show a maximum in the June solstice during the solar minimum years 2007–2009 (Figure 2 and Figure 3). This is in agreement with the results reported by the previous researchers [*Burke et al*., 2004a, 2004b, *Huang et al*., 2014; *Liu et al*., 2015]. Using GPS data, *Liu et al*. [2015] conducted an analysis of plasma bubbles over the Sanya region, at similar latitude as the Hong Kong. They reported two clear seasonal maxima in scintillation (S_4) and significant TEC fluctuation (ROTI), corresponding to the spring (March–April) and autumn (September–October) equinoctial months, only except during the solar minimum years in 2008–2009. Moreover, during 2008–2009, they have reported scintillation maxima in June. Using the data from the Communications/Navigation Outage Forecasting System (C/NOFS) satellite, the occurrence probability of equatorial ionospheric irregularities measured during the period of low and moderate solar activity from 2008 to 2012, has been studied by *Huang et al*. [2014]. They reported the high occurrence probability during June solstice of low solar activity years 2008–2010 at African-Asian-Pacific longitudes. Using the data from Defense Meteorological Satellite Program (DMSP), *Burke et al*. [2004a, 2004b] have shown that EPB occurrences are more common during northern summer (June–August) for the longitudes where geomagnetic equator resides in the northern hemisphere, whereas the same is more common during southern summer (December–February) for the longitudes where geomagnetic equator resides in southern hemisphere. Moreover, the difference in longitude trend of EPB occurrences over American and Asian longitudes could not be predicted by model proposed by *Tsunoda* [1985]. The seasonal maximum occurrences of ionospheric irregularities are mainly governed by two parameters: one is postsunset rise of *F* layer (or vertical drift) due to PRE and other is seed

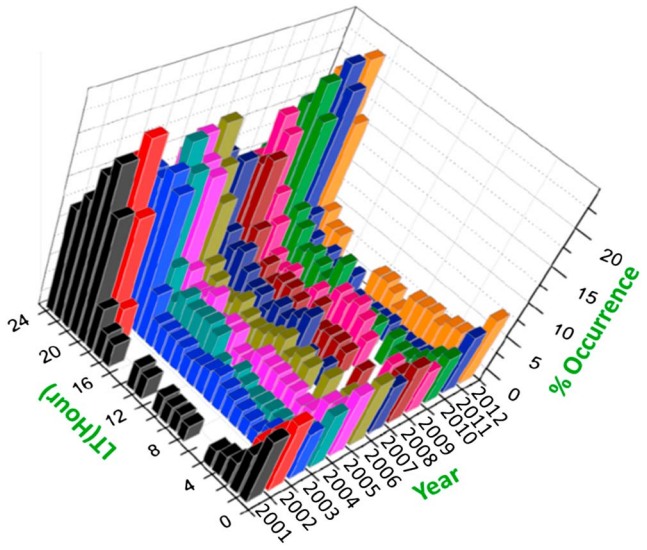

Figure 4. EPB occurrences (%) against Hong Kong local time from 2001 to 2012. The EPB occurrence is more frequent during nighttime than that during daytime throughout 2001–2012.

perturbation in plasma density induced by gravity waves from tropospheric origin. During low solar activity years, the vertical drift due to PRE is less significant and seed perturbation can control the seasonal variation of ionospheric irregularities and make their occurrences maximum during solstice months [*Tsunoda*, 2010]. The displacement between geographic and geomagnetic equator also plays an important role in controlling the seasonal/longitudinal variation of ionospheric irregularities [*Heelis et al.*, 2010]. Using the data from C/NOFS, *Heelis et al.* [2010] presented the global occurrence frequency of plasma irregularities. Their result was approximately in agreement with the proposed concept, i.e., high occurrence rate in the northern summer in a longitude sector of −30° to 120° where the magnetic equator is located in the northern hemisphere. They further suggested that the seasonal variation of irregularities particularly during low solar activity is influenced by the seeding which originates from the source in the troposphere and responds to the proximity of inter tropical convergence zone (ITCZ) to the magnetic equator. ITCZ is the region in the troposphere where gravity waves are supposed to be generated by mesoscale convective systems (MCSs). Although the results of *Huang et al.* [2014], for low solar activity years, over African-Asian-Pacific sectors are similar to our results over Hong Kong sector but the difference in relationship between the geographic and geomagnetic coordinates in Hong Kong sector in comparison to African-Pacific sector is noticed. The difference in relation between two regions may affect the results of drift and seeding perturbation, which in turn can affect the depth of EPBs. In addition, during the June solstice, several meteorological phenomena such as cyclones, typhoons, and hurricanes are dominant in the lower atmosphere/troposphere, around Hong Kong, and can play a significant role in triggering the plasma bubbles occurrences by generating gravity waves [*Bishop et al.*, 2006; *Kim et al.*, 2014]. These gravity waves generated in the lower atmosphere can propagate in a slant direction toward the ionosphere and trigger the growth of plasma bubbles[*Abdu et al.*, 2009; *Takahashi et al.*, 2009; *Taori et al.*, 2011].

EPBs during the March equinox have a higher value than during the September equinox throughout 2001–2012 except for the high solar activity year in 2001 (Figures 2 and 3). Whereas for 2001, the September equinox shows higher EPB occurrences than the March equinox. Thus, both the monthly as well as seasonal observed EPBs show equinoctial asymmetry throughout 2001–2012. The asymmetry in EPB occurrences could be caused by the suppression of the growth rate of instability by interhemispheric neutral winds, which is known to be a primary cause for triggering EPB or Equatorial Spread-F (ESF) [*Maruyama and Matuura*, 1984]. Using the numerical simulation, *Maruyama* [1988] showed that the role of interhemispheric neutral winds, which is directed from the summer hemisphere to the winter hemisphere, is to increase the Pedersen conductivity and thereby reduce the growth rate of the R-T instability. Using the data from GPS, *Sripathi et al.* [2011] have shown the equinoctial asymmetry in scintillation occurrence over the Indian region. They further argued that asymmetry in the electron density distribution and the meridional winds could be responsible for the equinoctial asymmetry in scintillation occurrences.

To study local time occurrences of EPB, we have analyzed the percentage of EPB occurrences against 00:00–24:00 local time hour for each year from 2001 to 2012 which is shown by the bar diagram in Figure 4. Generally, EPB occurrences are the most frequent during nighttime hours (19:00–24:00 h) than the daytime throughout 2001–2012. Apart from the nighttime, the daytime EPB have also been observed throughout 2001–2012 except during the high solar activity year 2002. The diurnal occurrence of EPB is found in agreement with those reported in previous works [*Rama Rao et al.*, 2006a, 2006b; *Nishioka et al.*, 2008].

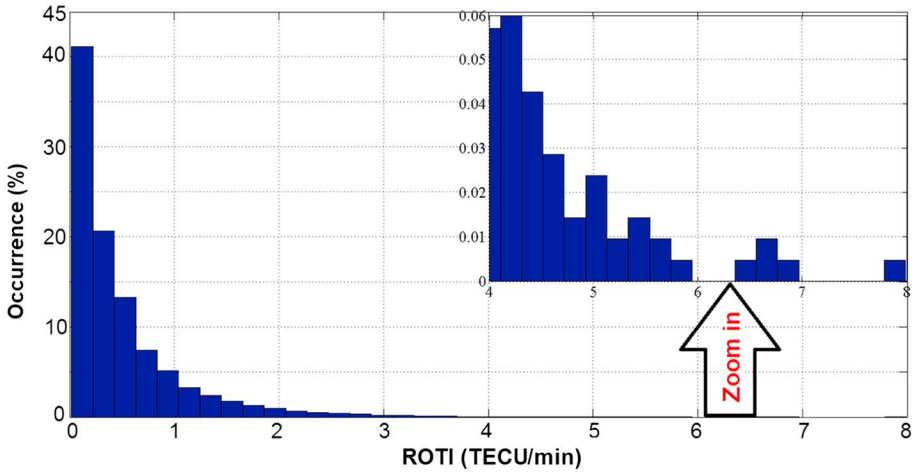

Figure 5. Percentage distribution of different rates of TEC change indices (ROTI) during 2001–2012. Generally, the ROTI is found to vary from 0 to 8 TECU/min but most ROTI are less than 1 TECU/min.

Unlike the nighttime occurrences of plasma bubble, the daytime occurrences also happen but such cases are very rare. It is known from earlier studies that the daytime plasma density irregularities are possibly caused by the sporadic *E* layers (E_s) associated irregularities [*Patra et al*., 2012; *Chatterjee et al*., 2013]. Using the spread-*F* data from Alouette I ionograms, *Dyson* [1977] has found a small but significant percentage of occurrences of plasma bubbles between local sunrise and noon times. The statistical analysis made by earlier researchers indicates that the favorable conditions for daytime EPBs occurrences are to be any one of the following: at early morning, at low latitude, at high altitude, and during geomagnetic storms [*Park et al*., 2015]. In addition, the daytime EPBs prefer higher altitude because of two factors: (i) daytime EPBs are leftover from nighttime/presunrise and (ii) EPBs at higher altitude are protected from the refilling due to daytime photoionization [*Huang et al*., 2013]. Using the data from radar observation, two afternoon EPBs above 600 km altitude, at Jicamarca, were reported during geomagnetic quiet periods [*Woodman et al*., 1985].

Apart from diurnal distribution of plasma bubbles, we have also analyzed the rate of TEC change index (ROTI) for the period 2001–2012. Figure 5 shows the percentage distributions of all the observed bubbles with different ROTI. In the upper right corner, we have shown the enlarged portion with ROTI larger than 4 TECU/min (1 TECU is equivalent to approximately 16 cm range for GPS L1 signal). We can see that generally, the ROTI varies 0–8 TECU/min but most ROTI are less than 1 TECU/min. An index to observe plasma bubble activity is the differential value of ROTI between evening and daytime ($\mathrm{ROTI}_{\mathrm{evening}} - \mathrm{ROTI}_{\mathrm{day}}$) and is discussed in detail by *Nishioka et al*. [2008]. A threshold of 0.075 TECU/min is generally used to indicate obvious scintillation effect on GPS signal. Based on the threshold criterion and occurrences of ROTI as seen from Figure 5, it is found that more than 75% of all observed plasma bubbles have the scintillation effects on the GPS signal.

3.2. Effect of Solar Activity

To study the effect of solar activity on the occurrence of EPB, the number of EPB occurrences observed during daytime, nighttime, and total EPB (day + night) along with sunspot number (SSN) has been plotted each year during 2001–2012, which is shown in Figures 6a and 6b. From this figure it is seen that the observed EPB (both day and night) varies in accordance with SSN and are found to be a maximum during the solar maximum year 2002 and a minimum during the solar minimum year 2008. Figures 6c and 6d, respectively, show the correlation analysis of total annual EPB occurrences with annual mean SSN and $F_{10.7}$ cm flux. To study the solar activity effect in more detail, the correlation analysis of monthly EPB occurrence against monthly mean SSN as well as solar $F_{10.7}$ cm flux has been carried out, which is shown in Figure 7. The correlation coefficient of monthly EPB occurrences to monthly mean SSN and $F_{10.7}$ cm flux are found to be 0.60 and 0.63, respectively. To study the seasonal impacts of solar activity on EPB occurrences, the correlation analysis has been carried out for the summer months (May to August), winter months (January, February, November, and December), and equinox months (March, April, September, and October). The seasonal analysis shows that EPBs are influenced more during the equinox ($R = 0.80$) than summer ($R = 0.62$) and winter ($R = 0.68$) season.

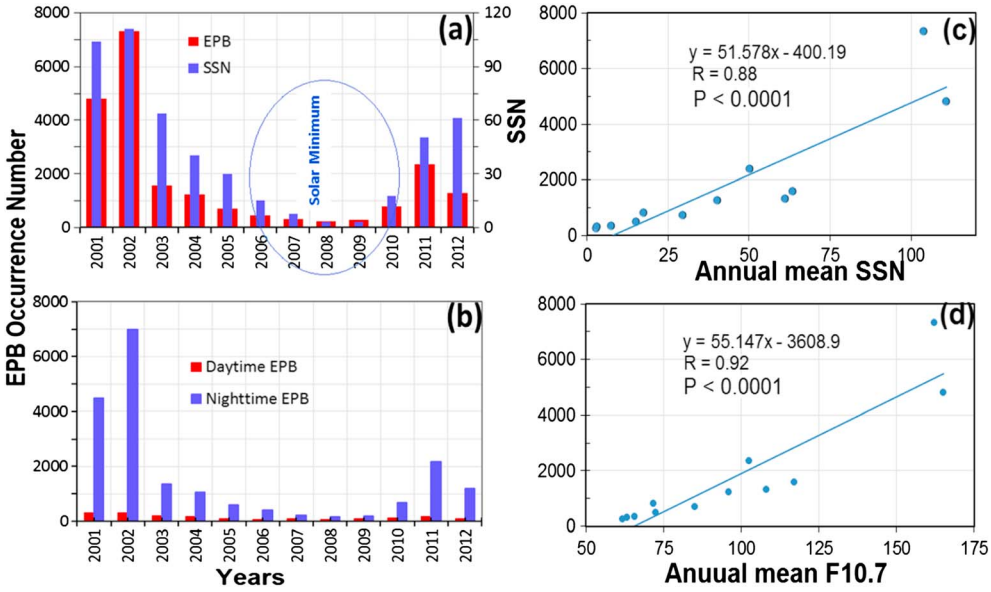

Figure 6. (a) Annual total EPB occurrences number observed over Hong Kong during 2001–2012 along with annual mean total sunspot number (SSN); (b) annual daytime and nighttime EPB occurrences number; (c) scatterplot showing the correlation between annual total EPB occurrences number and annual mean SSN; and (d) scatterplot showing the correlation between annual total EPB occurrences number and annual mean $F_{10.7}$ cm solar flux. The correlation coefficients (R) along with significance level (P) of the two data sets are mentioned.

The statistical test for the significance of relationships between two data set EPB occurrences and solar activity indices (SSN and $F_{10.7}$ cm flux) has also been carried out, and the significance level (P) has also been computed. The small of significance value ($P < 0.0001$) between EPB occurrences and solar activity (SSN and $F_{10.7}$ cm flux) indicates a strong correlation. Moreover, the impacts of solar activity on EPB occurrences vary more obviously on an annual basis than a monthly basis. The annual correlation of EPB occurrences with annual SSN and $F_{10.7}$ cm flux are found to be 0.88 and 0.92, respectively (Figures 6c and 6d). Furthermore, it is also observed that the EPB occurrence shows slightly more dependence on $F_{10.7}$ cm flux than SSN, which is evident from the computed significance level (P) and correlation coefficient. This confirms that the solar activity plays a major role in EPB occurrences, and more EPB can be expected during the solar maxima than solar minima [*Basu et al*., 2002].

More plasma bubble occurrences are observed in the high solar activity years than low solar activity years as can be seen from Figure 6. Since evening equatorial upward plasma drift due to prereversal enhancement (PRE), drifting is an important factor controlling the EPB occurrences, which varies with solar activity. Therefore, higher altitude plasma bubbles are observed during high solar activity years than that during low solar activity years. Using both observation and model data, *Vichare and Richmond* [2005] and *Fejer et al*. [2008] have shown a linear correlation of the evening equatorial upward plasma drift with solar flux level. Furthermore, *Stolle et al*. [2008] and *Su et al*. [2008] have presented global evidence for the linear relationship between the EPB occurrence rate and the vertical plasma drift.

We have observed that the effects of solar activity on EPB occurrences are more obvious in annual basis than monthly basis and have an annual correlation of 0.92 between annual EPB occurrences and annual mean $F_{10.7}$ cm flux. Moreover, the effects of solar activity are seasonal, achieving maximum during the equinox. Our results are in agreement with those reported in previous works [*Huang et al*., 2001, 2002; *Sobral et al*., 2002; *Chu et al*., 2005; *Nishioka et al*., 2008]. Using data from DMSP, *Huang et al*. [2002] showed that the annual mean $F_{10.7}$ cm flux correlates very well with EPB occurrence ($R = 0.98$) along all longitude sectors. In previous studies it was shown that influence of solar activity on EPB occurrences depends on season [*Sobral et al*., 2002; *Chu et al*., 2005]. For the Brazilian sector, using the data from airglow observations during a 22 year period from 1977 to 1998, *Sobral et al*. [2002] have shown that the solar activity impacts on EPB are more noticeable during the equinox months. Using GPS data, *Nishioka et al*., 2008 have shown that the effects of solar activity on EPBs are different for different longitude sector and reported highest correlation for

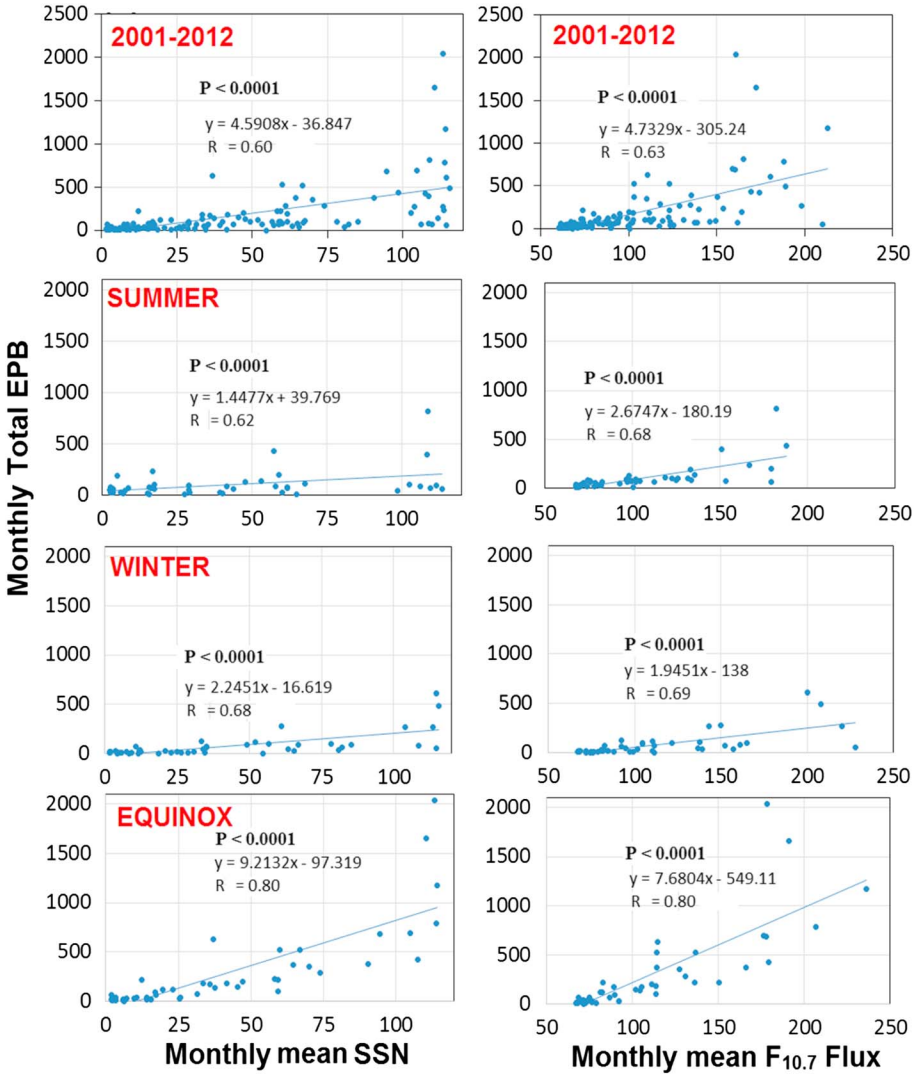

Figure 7. Scatter plot showing the correlation between monthly total EPB occurrences and solar activity parameters (left column: SSN; right: $F_{10.7}$ cm flux) during 2001–2012. The correlation coefficients (R) along with significance level (P) of the two data sets are mentioned.

African-Asian sector. They further reported a poor correlation between solar activity and EPBs for Atlantic sector, which is in contrast to our result in Hong Kong sector. *Burke et al.* [2004b] pointed out that the South Atlantic Anomaly could be responsible for the lack of a clear solar cycle dependence of EPB occurrences in the Atlantic sector, because EPB generation in this sector may be influenced by inner magnetospheric particle precipitation. In addition, the influences of solar activity on EPB occurrences are further complicated by observation techniques and can cause conflicting interpretation of the EPB climatology [e.g. *Miller et al.*, 2010; *Makela and Miller*, 2011]. *Makela and Miller* [2011] have shown that solar cycle dependence of EPB is significantly different between their ground-based airglow and in situ DMSP measurements.

3.3. Effect of Magnetic Activity

To study the impact of magnetic activity on EPB occurrence, we have selected a strong geomagnetic storm with $Dst_{\text{minimum}} = -221$ nT which commenced on 24 November 2001. The variation of other geomagnetic parameters such as *SYM-H* index, IMF B_z, IEF E_y, and *AE* index against UT hours during 24–27 November 2001 is shown in Figure 8. This figure shows that the storm commenced at 06:16 UT (Hong Kong local time = UT + 8 h) with two minima in *SYM-H* index at around 08:16 (−130 nT) and 12:66 UT (−233 nT) on 24 November. After this, *SYM-H* started to recover to become quiet time value on 27 November. On 24

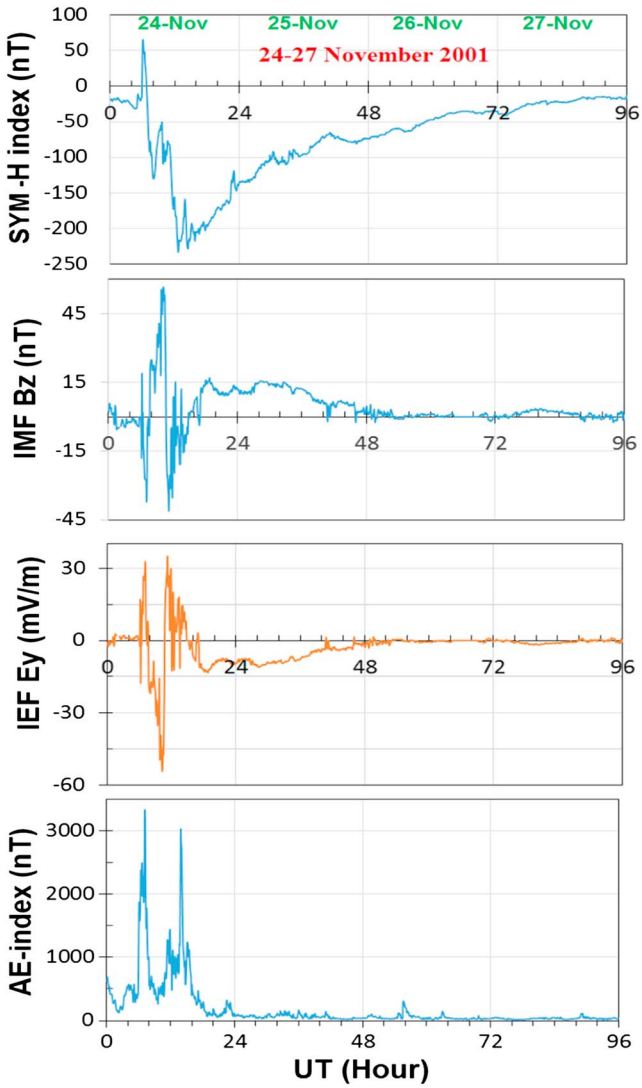

Figure 8. Variation of symmetric ring current (*SYM-H*) index, *z* component of interplanetary magnetic field (IMF B_z), *y* component of interplanetary electric field (IEF E_y) and auroral electrojet (*AE*) index during 24–27 November 2001. The reduction in SYM-H index as low as −233 nT on 24 November 2001 indicates the strong geomagnetic storm activity.

November 2001 IMF B_z turned southward at around 06:25 UT and remained so till 07:06 UT with a minimum value of −37.16 nT. During this period IEF E_y turned eastward at 06:30 UT and showed a maximum value of 32.81 mV/m at around 07:06 UT. After 07:06 UT IMF B_z turned northward and remained so till 10:18 UT. During this period the IEF E_y became westward at 07:15 UT and showed a maximum value of −54 mV/m at around 10:15 UT.

The prompt penetration electric field (PPE) arises due to the under shielding and over shielding conditions, divergence of the asymmetric ring currents, and enhanced polar cap potential drop [*Fejer et al.*, 2007]. The sudden southward turning of IMF B_z, from a steady northward configuration, produces a dawn to dusk convection electric field at high latitudes [*Kikuchi et al.*, 2008]. This creates the so-called undershielding condition and the electric field penetrates instantaneously to the equatorial and low latitudes. However, after a steady southward configuration, the IMF Bz turns northward again and the overshielding condition occurs. It operates on time scales of an hour or so [*Fejer et al.*, 2007; *Kumar and Singh*, 2011a, 2011b]. During the daytime PPE is eastward and enhances the dynamic electric field which enhances vertical $E \times B$ plasma drift lifting the plasma to higher altitudes [*Rastogi and Klobuchar*, 1990].

To observe the effect of storm-induced electric field on ionosphere, the variation of VTEC along with quiet mean VTEC estimated during seven quiet days of November 2001 is depicted in Figure 9. As noted from the figure, a depression in VTEC observed from 00:00 to 08:00 UT and then a small enhancement until around 10:00 UT on 24 November. After 10:00 UT VTEC again started decreasing until 11:15 UT. The depression in VTEC indicates the downward drift of the *F* region ionosphere which was caused by westward turning of penetration electric field. At 10:25 UT IMF B_z turned southward again and remained so till 11:15 UT which resulted in eastward turning of IEF E_y at 10:26 UT and peak value of 35 mV/m at around 11:15 UT. Due to this eastward electric field, VTEC started to increase at several GPS stations in Hong Kong from 11:18 to 14:00 UT and showed a maximum VTEC enhancement of 25 TECU at around 13:57 UT (Figure 9). On 24 November, IEF E_y (penetration electric field) became eastward and showed peaks at 07:06 and 11:15 UT. This eastward electric field could cause the upward lift to the *F* layer of the ionosphere via $E \times B$ plasma drift and producing a favorable situation for the excitation of the R-T instability [*Fejer et al.*, 1999]. The upward $E \times B$ drift in ionosphere could also result in VTEC enhancement and can be seen from Figure 9.

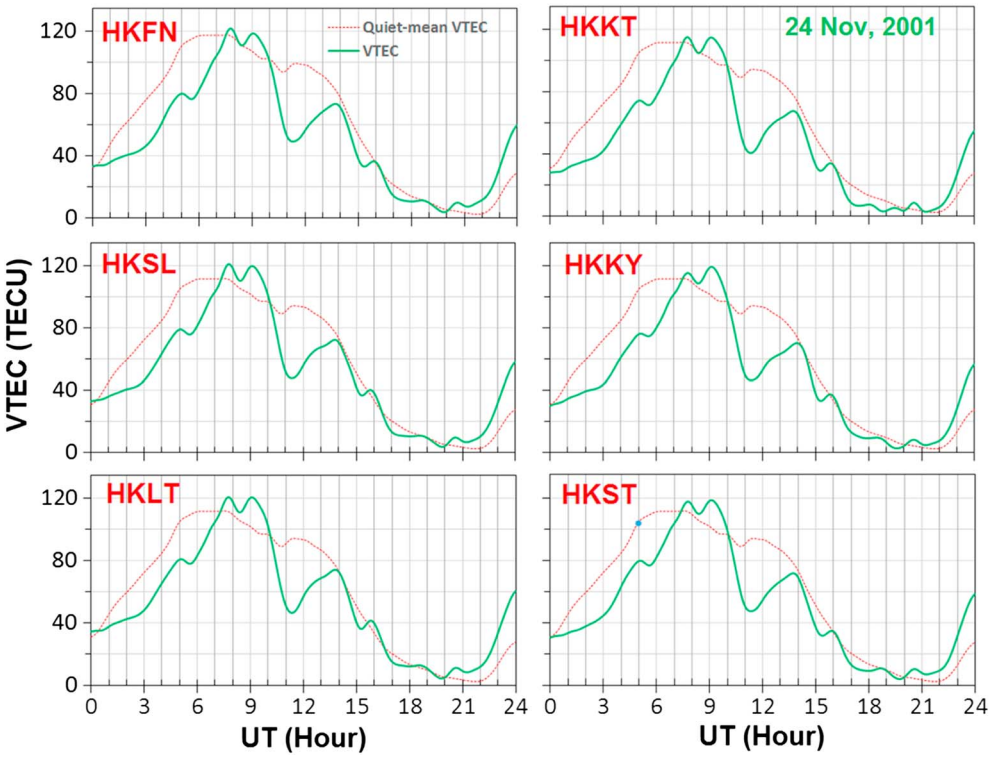

Figure 9. Variation of VTEC on storm day 24 November 2001 and quiet mean VTEC estimated during quiet days of November 2001 over six different stations in Hong Kong. The quiet mean VTEC has been computed by averaging the VTEC during seven quiet days of November 2001.

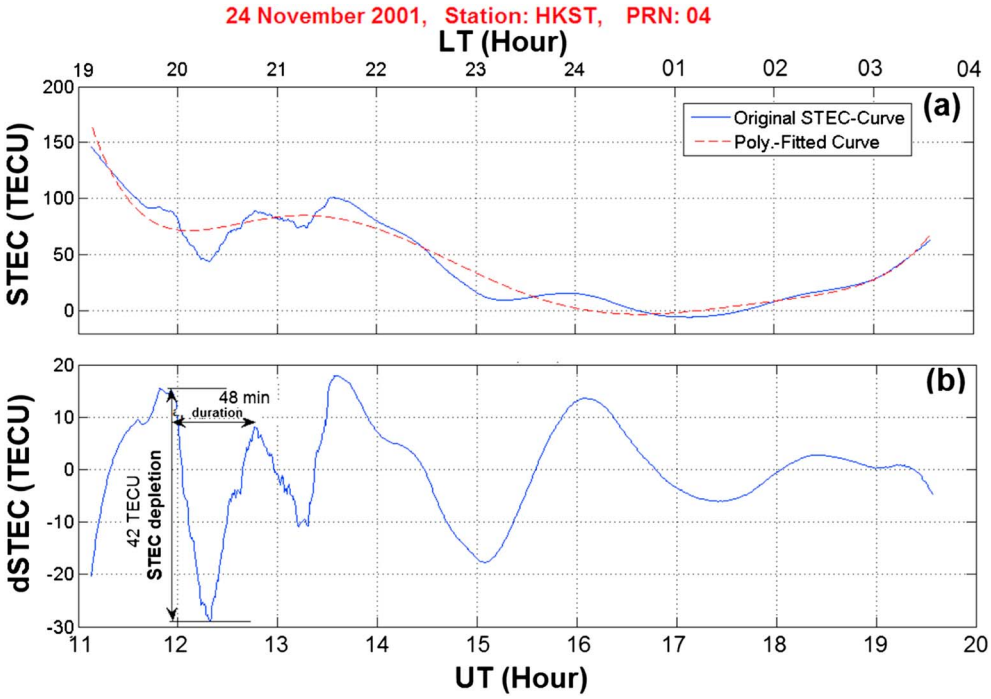

Figure 10. Time series of original STEC and best polynomial fitted curve observed by PRN 04 at HKST station, Hong Kong during geomagnetic storm on (a) 24 November 2001; (b) the time series of detrended of STEC (dSTEC) showing characteristics of the Plasma bubble.

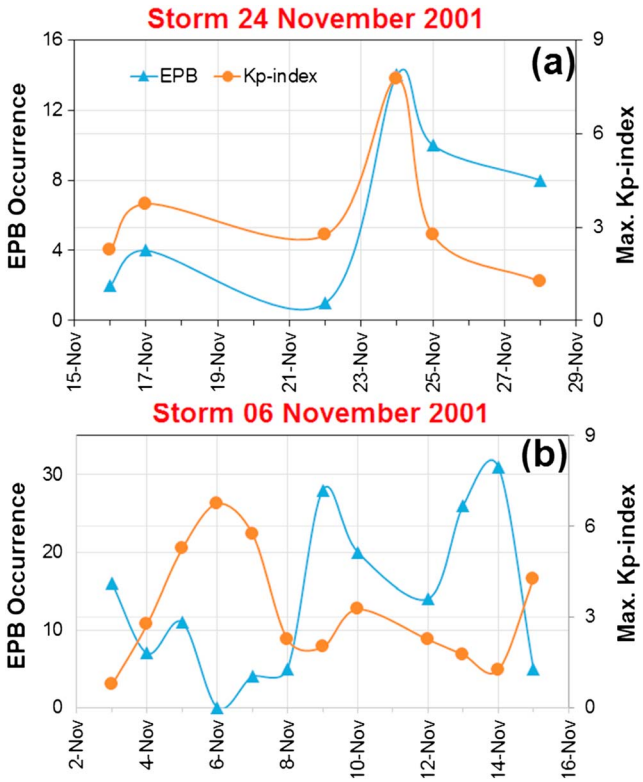

Figure 11. EPB occurrence along with daily maximum *Kp* index during few days before and after the geomagnetic storm (a) for 24 November 2001 and (b) for 6 November 2001.

The enhancement of VTEC is seen between 11:30 and 14:00 UT and formed the second peak in VTEC at around 13:57 UT. During this enhancement IEF E_y was westward and PPE cannot produce such enhancement. The other probability is disturbance dynamoelectric field (DDE) which can be generated by geomagnetic storm due to modification of neutral wind circulation at high latitudes. At the equator, the direction of DDE is westward during the daytime and eastward during the nighttime [*Zhao et al*., 2005]. But the direction of the zonal ambient electric field is eastward during the daytime and westward during the nighttime. The ionospheric perturbation due to effect of DDE can be sensed over time scales of some hours to days after the geomagnetic storms [*Scherliess and Fejer*, 1997; *Fuller-Rowell et al*., 2002]. As VTEC enhancement has been observed during 11:30–14:00 UT (19:30–22:00 LT), it could be caused by the DDE, because the direction of DDE is eastward during nighttime and can produce upward plasma drift [*Maruyama et al*., 2005], i.e., a favorable condition for the excitation of R-T instability or growth of plasma bubble. Using multilocation GPS observations, *Cherniak et al*. [2015] studied the dynamics of high-latitude ionospheric irregularities during the geomagnetic storm on 17 March 2015 and showed that significant increases in the intensity of the irregularities within the polar cap region of both hemispheres were associated with the formation and evolution of storm enhanced density (or TEC) of ionization structures and polar patches. We have observed three successive strong plasma bubble occurrences from 12:00 to 15:40 UT on 24 November 2001, as shown in Figure 10. To see the impacts of magnetic activity on EPB occurrence during this storm period, we have also analyzed the daily EPB occurrence along with the daily maximum value of *Kp* index a few days before and after 24 November 2001, which is shown in Figure 11a. It is clearly seen from this figure that there is a one-to-one correspondence between magnetic activity and EPB occurrence. Moreover, the magnetic activity enriches the EPB occurrence. The development of plasma bubbles in the evening sector during the early stages of high magnetic activities has been observed by *Huang et al*. [2001, 2002], which suggests that penetration electric fields during southward IMF are responsible for driving plasma bubbles. Using the data from the Defense Meteorological Satellite Program (DMSP) satellite, *Huang et al*. [2010] found that the penetration electric field at dusk is eastward, lasting for several hours during the main phase of magnetic storms and causing large upward ion drift in the equatorial ionosphere.

We have also considered another geomagnetic storm that commenced in postmidnight sector at 20:00 UT on 5 November 2001 (i.e., 04:00 LT on 6 November). The storm's main phase ended at 07:00 UT on 6 November ($Dst_{minimum} = -292$ nT). For this storm, the other geomagnetic parameters (IMF B_z and IEF E_y) are not completely available on the website. The daily EPB occurrence along with daily maximum value of *Kp* index during a few days before and after 6 November 2001 is shown in Figure 11b. From this figure it is clear that magnetic activity suppresses EPB occurrence and no EPB is observed on storm day, i.e., 6 November 2001. Our result is found to be in agreement with those reported in earlier works, which showed suppression of EPB during strong geomagnetic storm around the midnight/postmidnight sector [*Oya et al*., 1986; *Singh et al*., 1997;

Huang, 2011]. Since the commencement of this storm is at local nighttime (04:00 LT), therefore PPE is opposite to ambient electric field and cannot enhance the vertical $E \times B$ plasma drift. It is known that the low-latitude ionosphere can be sensitive to DDE effect 3–4 h after the geomagnetic storm. Therefore, for the storm of 6 November, DDE can be expected to operate in daytime hours and is westward so it cannot trigger upward plasma drift and consequently suppressed the EPB occurrences.

4. Conclusions

The occurrence and characteristics of plasma bubbles during 2001–2012, which is more than a complete solar cycle, have been studied using STEC data from the SatRef GPS CORS network in Hong Kong. The plasma bubbles have the maximum occurrences during equinox months throughout the years except the low solar activity period 2007–2009. During 2007–2008, the EPB occurrences are found to be a maximum during June solstice. For 2009, the EPB occurrences during June solstice are found to be even larger than the September equinox but slightly smaller than the March equinox. The high occurrences of EPB during June solstice of solar minimum 2007–2009, which were observed over Hong Kong using local GPS CORS network, is a significant finding of this study. The satellite-based observation reported by *Huang et al*. [2014] over African-Asian-Pacific longitudes during low solar activity period 2008–2010 is in agreement with our results which have been observed with ground-based observation from GPS. However, the difference in relationship between the geographic and geomagnetic coordinates in two regions could affect the depth of the plasma bubbles which needs further investigation. The equinoctial asymmetry in EPB occurrences was observed throughout 2001–2012. The asymmetry in the EPB occurrences could be caused by the suppression of the growth rate of the instability by interhemispheric neutral winds, which is known to be a primary cause for triggering EPB or ESF. Generally, EPB occurrences are found to be at maximum during the nighttime hours (19:00–24:00 h in local time). Apart from the nighttime, daytime occurrences of EPB are also observed with maximum daytime occurrences during high solar activity year.

The influence of solar activity on EPB occurrences is studied via correlation analysis, and the correlations are different in different seasons with a maximum in the equinox season. Moreover, the EPB occurrences show a larger correlation with $F_{10.7}$ flux than that with the SSN. The seasonal impact of solar activity on EPB occurrences over the Hong Kong region is found in agreement with those reported in the Brazilian sector [*Sobral et al*., 2002; *Chu et al*., 2005] but different to that in Atlantic sector [*Nishioka et al*., 2008]. The South Atlantic Anomaly (SAA) could be responsible factor for the lack of a clear solar cycle dependence of EPB occurrences in the Atlantic sector, as EPB generation in this sector may be influenced by inner magnetospheric particle precipitation [*Burke et al*., 2004b].

To study the impact of magnetic activity on EPB occurrences, two cases of geomagnetic storms have been considered. The geomagnetic storms were observed on 6 November 2001 and 24 November 2001, respectively. It was found that the impact of storms on EPB occurrences is local time dependent on storm occurrences. The storm on 24 November 2001 in the evening sector triggers the EPB occurrence, whereas the storm on 6 November 2001 in the postmidnight sector suppresses the EPB occurrence.

Acknowledgments

The geomagnetic data have been taken from world data center at Kyoto University, Japan (http://wdc.kugi.kyoto-u.ac.jp/) and solar data (SSN and $F_{10.7}$ cm flux) from NOAA's National Centers for Environmental Information (http://www.ngdc.noaa.gov). The Hong Kong Research Grants Council (RGC) (projects PolyU 152023/14E, PolyU 5325/12E F-PP0F, and PolyU 5203/13E B-Q37X) and the National Natural Science Foundation of China (41274039) are cordially acknowledged for financial assistance. The Lands Department of the Government of Hong Kong Government of Special Administrative Region (HKSAR) and the Cartography and Cadastre Bureau (DSCC) of Macao Government of Special Administrative Region (Macao SAR) are thanked for providing GNSS data for this work from the Hong Kong Satellite Positioning Reference Station Network (SatRef) and Macao Reference Network, respectively. The data used in this paper are available with Wu Chen and Sanjay Kumar (e-mails: lswuchen@polyu.edu.hk; sanjay.skitvns@gmail.com). SK is thankful to SERB, New Delhi for support (SR/FTP/ES-164/2014). Authors are thankful to the reviewers for their valuable comments/suggestions which are very helpful to improve the manuscript's quality.

References

Aarons, J. (1991), The role of the ring current in the generation or inhibition of equatorial *F* layer irregularities during magnetic storms, *Radio Sci.*, *26*, 1131–1149, doi:10.1029/91RS00473.

Aarons, J. (1993), The longitudinal morphology of equatorial F-layer irregularities relevant to their occurrence, *Space Sci. Rev.*, *63*, 209–243.

Abdu, M. A. (2001), Outstanding problems in the equatorial ionosphere thermosphere electrodynamics relevant to spread F, *J. Atmos. Sol. Terr. Phys.*, *63*, 869–884, doi:10.1016/S1364-6826(00)00201-7.

Abdu, M. A., J. H. A. Sobral, I. S. Batista, V. H. Rios, and C. Medina (1998), Equatorial spread-F occurrence statistics in the American longitudes: Diurnal, seasonal and solar cycle variations, *Adv. Space Res.*, *22*(6), 851–854, doi:10.1016/S0273-1177(98)00111-2.

Abdu, M. A., E. Alam Kherani, I. S. Batista, E. R. de Paula, D. C. Fritts, and J. H. A. Sobral (2009), Gravity wave initiation of equatorial spread F/plasma bubble irregularities based on observational data from the SpreadFEx campaign, *Ann. Geophys.*, *27*(7), 2607–2622, doi:10.5194/angeo-27-2607-2009.

Basu, S., and S. Basu (1985), Equatorial scintillations: Advances since ISEA-6, *J. Atmos. Terr. Phys.*, *47*, 753–768, doi:10.1016/0021-9169(85)90052-2.

Basu, S., E. MacKenzie, and S. Basu (1988), Ionospheric constraints on VHF/UHF communication links during solar maximum and minimum periods, *Radio Sci.*, *23*, 363–378, doi:10.1029/RS023i003p00363.

Basu, S., K. M. Groves, S. Basu, and P. J. Sultan (2002), Specification and forecasting of scintillations in communication/navigation links: Current status and future plans, *J. Atmos. Sol. Terr. Phys.*, *64*, 1745–1754, doi:10.1016/S1364-6826(02)00124-4.

Bishop, R. L., N. Aponte, G. D. Earle, M. Sulzer, M. F. Larsen, and G. S. Peng (2006), Arecibo observations of ionospheric perturbations associated with the passage of Tropical Storm Odette, *J. Geophys. Res.*, *111*, A11320, doi:10.1029/2006JA011668.

Burke, W. J., C. Y. Huang, L. C. Gentile, and L. Bauer (2004a), Seasonal longitudinal variability of equatorial plasma bubbles, *Ann. Geophys.*, *22*, 3089–3098, doi:10.5194/angeo-22-3089-2004.

Burke, W. J., L. C. Gentile, C. Y. Huang, C. E. Valladres, and S. Y. Su (2004b), Longitudinal variability of equatorial plasma bubbles observed by DMSP and ROCSAT-1, *J. Geophys. Res.*, *109*, A12301, doi:10.1029/2004JA010583.

Carter, B. A., et al. (2014), Geomagnetic control of equatorial plasma bubble activity modeled by the TIEGCM with Kp, *Geophys. Res. Lett.*, *41*, 5331–5339, doi:10.1002/2014GL060953.

Chakraborty, S. K., A. Dasgupta, S. Roy, and S. Banerjee (1999), Long-term observations of VHF scintillations and total electron content near the crest of the equatorial anomaly in the Indian longitude zone, *Radio Sci.*, *34*, 241–255, doi:10.1029/98RS02576.

Chatterjee, S., S. K. Chakraborty, and S. Majumdar (2013), Summer time scintillations near the transition zone of the Indian longitude sector, *J. Atmos. Sol. Terr. Phys.*, *95–96*, 102–115, doi:10.1016/j.jastp.2013.01.017.

Chen, W., S. Gao, C. Hu, Y. Chen, and X. Ding (2008), Effects of ionospheric disturbance on GPS observation in low latitude area, *GPS, Sol.*, *12*(1), 33–41.

Cherniak, I., I. Zakharenkova, and R. J. Redmon (2015), Dynamics of the high-latitude ionospheric irregularities during the 17 March 2015 St. Patrick's Day storm: Ground-based GPS measurements, *Space Weather*, *13*, 585–597, doi:10.1002/2015SW001237.

Chu, F. D., J. Y. Liu, H. Takahashi, J. H. A. Sobral, M. J. Taylor, and A. F. Medeiros (2005), The climatology of ionospheric plasma bubbles and irregularities over Brazil, *Ann. Geophys.*, *23*, 379–384, doi:10.5194/angeo-23-379-2005.

DasGupta, A., A. Maitra, and S. Basu (1981), Occurrence of nighttime VHF scintillations near the equatorial anomaly crest in the Indian sector, *Radio Sci.*, *16*(6), 1455–1458, doi:10.1029/RS016i006p01455.

Dyson, P. L. (1977), Topside irregularities in the equatorial ionosphere, *J. Atmos. Terr. Phys.*, *39*, 1269–1275.

Fejer, B. G., L. Scherliess, and E. R. de Paula (1999), Effects of the vertical plasma drift velocity on the generation and evolution of equatorial spread *F*, *J. Geophys. Res.*, *104*, 19,859–19,869, doi:10.1029/1999JA900271.

Fejer, B. G., J. W. Jensen, T. Kikuchi, M. A. Abdu, and J. L. Chau (2007), Equatorial ionospheric electric fields during the November 2004 magnetic storm, *J. Geophys. Res.*, *112*, A10304, doi:10.1029/2007JA012376.

Fejer, B. G., J. W. Jensen, and S.-Y. Su (2008), Quiet time equatorial *F* region vertical plasma drift model derived from ROCSAT-1 observations, *J. Geophys. Res.*, *113*, A05304, doi:10.1029/2007JA012801.

Fuller-Rowell, T. M., G. H. Miillward, A. D. Richmond, and M. V. Codrescu (2002), Storm time changes in the upper atmosphere at low latitudes, *J. Atmos. Sol. Terr. Phys.*, *64*, 1383–1391, doi:10.1016/S1364-6826(02)00101-3.

Heelis, R. A. (2004), Electrodynamics in the low and middle latitude ionosphere: A tutorial, *J. Atmos. Sol. Terr. Phys.*, *66*, 825–838, doi:10.1016/j.jastp.2004.01.034.

Heelis, R. A., R. Stoneback, G. D. Earle, R. A. Haaser, and M. A. Abdu (2010), Medium-scale equatorial plasma irregularities observed by Coupled Ion-Neutral Dynamics Investigation sensors aboard the Communication Navigation Outage Forecast System in a prolonged solar minimum, *J. Geophys. Res.*, *115*, A10321, doi:10.1029/2010JA015596.

Huang, C. Y., W. J. Burke, J. S. Machuzak, L. C. Gentile, and P. J. Sultan (2001), DMSP observations of equatorial plasma bubbles in the topside ionosphere near solar maximum, *J. Geophys. Res.*, *106*, 8131–8142, doi:10.1029/2000JA000319.

Huang, C. Y., W. J. Burke, J. S. Machuzak, L. C. Gentile, and P. J. Sultan(2002), Equatorial plasma bubbles observed by DMSP satellites during a full solar cycle: Toward a global climatology, *J. Geophys. Res.*, *107*(A12), 1434, doi:10.1029/2002JA009452.

Huang, C.-S., O. de La Beaujardiere, R. F. Pfaff, J. M. Retterer, P. A. Roddy, D. E. Hunton, Y.-J. Su, S.-Y. Su, and F. J. Rich (2010), Zonal drift of plasma particles inside equatorial plasma bubbles and its relation to the zonal drift of the bubble structure, *J. Geophys. Res.*, *115*, A07316, doi:10.1029/2010JA015324.

Huang, C.-S. (2011), Occurrence of equatorial plasma bubbles during intense magnetic storms, *Int. J. Geophys.*, 401858, doi:10.1155/2011/401858.

Huang, C.-S., O. de La Beaujardiere, P. A. Roddy, D. E. Hunton, J. O. Ballenthin, and M. R. Hairston (2013), Long-lasting daytime equatorial plasma bubbles observed by the C/NOFS satellite, *J. Geophys. Res., Space Physics*, *118*, 2398–2408, doi:10.1002/jgra.50252.

Huang, C.-S., O. de La Beaujardiere, P. A. Roddy, D. E. Hunton, J. Y. Liu, and S. P. Chen (2014), Occurrence probability and amplitude of equatorial ionospheric irregularities associated with plasma bubbles during low and moderate solar activities (2008–2012), *J. Geophys. Res., Space Physics*, *119*, 1186–1199, doi:10.1002/2013JA019212.

Iyer, K. N., M. N. Jivani, M. A. Abdu, H. P. Joshi, and M. Aggarwal (2006), Power spectral studies of VHF ionospheric scintillations near the equatorial anomaly in India, *Ind. J. Radio Space Phys.*, *35*, 234–241.

Ji, S., W. Chen, X. Ding, and C. Zhao (2011), Equatorial ionospheric zonal drift by monitoring local GPS reference network, *J. Geophys. Res.*, *16*, A08310, doi:10.1029/2010JA015993.

Ji, S., et al. (2013), A study of occurrence characteristics of plasma bubbles over Hong Kong area, *Adv. Space Res.*, *52*, 1949–1958, doi:10.1016/j.asr.2013.08.026.

Kelley, M. C. (2009), *The Earth's Ionosphere: Plasma Physics and Electrodynamics*, 2nd ed., Elsevier, London.

Kikuchi, T., K. K. Hashimoto, and K. Nozaki (2008), Penetration of magnetospheric electric fields to the equator during a geomagnetic storm, *J. Geophys. Res.*, *113*, A06214, doi:10.1029/2007JA012628.

Kim, S. H., H.-Y. Chun, and W. Jang (2014), Horizontal divergence of typhoon-generated gravity waves in the upper troposphere and lower stratosphere (UTLS) and its influence on typhoon evolution, *Atmos. Chem. Phys.*, *14*(7), 3175–3182, doi:10.5194/acp-14-3175-2014.

Kintner, P. M., B. M. Ledvina, E. R. de Paula, and I. J. Kantor (2004), Size, shape, orientation, speed, and duration of GPS equatorial anomaly scintillations, *Radio Sci.*, *39*, RS2012, doi:10.1029/2003RS002878.

Kumar, S., and A. K. Singh (2009), Variation of ionospheric total electron content in Indian low latitude region of equatorial ionization anomaly (EIA), *J. Adv. Space Res.*, *43*, 1555–1562, doi:10.1016/j.asr.2009.01.037.

Kumar, S., and A. K. Singh (2011a), Storm time response of GPS-derived total electron content (TEC) during low solar active period at Indian low latitude station Varanasi, *Astrophys. Space Sci.*, *331*, 447–458, doi:10.1007/s10509-010-0459-y.

Kumar, S., and A. K. Singh (2011b), GPS derived ionospheric TEC response to geomagnetic storm on 24 August 2005 at Indian low latitude stations, *Adv. Space Res.*, *47*, 710–717, doi:10.1016/j.asr.2010.10.015.

Langley, R., M. Fedrizzi, E. Paula, M. Santos, and A. Komjathy (2002), Mapping the low latitude ionosphere with GPS, *GPS World*, *13*(2), 41–46.

Li, G., B. Ning, L. Liu, W. Wan, and J. Y. Liu (2009), Effect of magnetic activity on plasma bubbles over equatorial and low-latitude regions in East Asia, *Ann. Geophys.*, *27*, 303–312.

Liu, K., G. Li, B. Ning, L. Hu, and H. Li (2015), Statistical characteristics of low-latitude ionospheric scintillation over China, *Adv. Space Res.*, *55*(5), 1356–1365, doi:10.1016/j.asr.2014.12.001.

Makela, J., and E. Miller (2011), Influences on the development of equatorial plasma bubbles: Insights from a long-term optical dataset, in *Aeronomy of the Earth's Atmosphere and Ionosphere*, *IAGA Spec. Sopron Book Ser.*, vol. 2, edited by M. A. Abduand D. Pancheva, pp. 239–249, Springer, Netherlands, doi:10.1007/978-94-007-0326-1_17.

Makela, J. J., B. M. Ledvina, M. C. Kelley, and P. M. Kinter (2004), Analysis of the seasonal variations of equatorial plasma bubble occurrence observed from Haleakala, Hawaii, *Ann. Geophys.*, *22*, 3109–3121, doi:10.5194/angeo-22-3109-2004.

Maruyama, N., A. D. Richmond, T. J. Fuller-Rowell, M. V. Codrescu, S. Sazykin, F. R. Toffoletto, R. W. Spiro, and G. H. Millward (2005), Interaction between direct penetration and disturbance dynamo electric fields in the storm-time equatorial ionosphere, *Geophys. Res. Lett.*, *32*, L17105, doi:10.1029/2005GL023763.

Maruyama, T. (1988), A diagnostic model for equatorial spread *F*: 1. Model description and application to electric field and neutral wind effects, *J. Geophys. Res.*, *93*, 14,611–14,622, doi:10.1029/JA093iA12p14611.

Maruyama, T., and N. Matuura (1984), Longitudinal variability of annual changes in activity of equatorial spread F and plasma bubbles, *J. Geophys. Res.*, *89*(A12), 10,903–10,912, doi:10.1029/JA089iA12p10903.

Mendillo, M., and J. Baumgardner (1982), Airglow characteristics of equatorial plasma depletions, *J. Geophys. Res.*, *87*(A9), 7641–7652, doi:10.1029/JA087iA09p07641.

Miller, E. S., J. J. Makela, K. M. Groves, M. C. Kelley, and R. T. Tsunoda (2010), Coordinated study of coherent radar backscatter and optical airglow depletions in the central Pacific, *J. Geophys. Res.*, *115*, A06307, doi:10.1029/2009JA014946.

Nishioka, M., A. Saito, and T. Tsugawa (2008), Occurrence characteristics of plasma bubble derived from global ground-based GPS receiver networks, *J. Geophys. Res.*, *113*, A05301, doi:10.1029/2007JA012605.

Oya, H., T. Takahashi, and S. Watanabe (1986), Observation of low latitude ionosphere by the impedance probe on board the Hinotori Satellite, *J. Geomagn. Geoelectr.*, *38*, 111–123, doi:10.5636/jgg.38.111.

Park, J., C. Stolle, C. Xiong, H. Lühr, R. F. Pfaff, S. Buchert, and C. R. Martinis (2015), A dayside plasma depletion observed at mid latitudes during quiet geomagnetic conditions, *Geophys. Res. Lett.*, *42*, 967–974, doi:10.1002/2014GL062655.

Patil, P. T., et al. (2016), The study of equatorial plasma bubble during January to April 2012 over Kolhapur (India), *Ann. Geophys.*, *59*(2, A0214).

Patra, A. K., P. P. Chaitanya, and A. Bhattacharyya (2012), On the nature of radar backscatter and 250 MHz scintillation linked with an intense daytime E_s patch, *J. Geophys. Res.*, *117*, A03315, doi:10.1029/2011JA016981.

Pi, X., A. J. Mannucci, U. J. Lindqwister, and C. M. Ho (1997), Monitoring of global ionospheric irregularities using the Worldwide GPS Network, *Geophys. Res. Lett.*, *24*(18), 2283–2286, doi:10.1029/97GL02273.

Portillo, A., M. Herraiz, S. M. Radicella, and L. Ciraolo (2008), Equatorial plasma bubbles studied using African slant total electron content observations, *J. Atmos. Sol. Terr. Phys.*, *70*, 907–917, doi:10.1016/j.jastp.2007.05.019.

Rama Rao, P. V. S., S. Tulasi Ram, S. Gopi Krishna, K. Niranjan, and D. S. V. V. D. Prasad (2006a), Morphological and spectral characteristics of L-band and VHF scintillations and their impact on transionospheric communications, *Earth Planets Space*, *58*, 895–904, doi:10.1186/BF03351994.

Rama Rao, P. V. S., S. Gopi Krishna, K. Niranjan, and D. S. V. V. D. Prasad (2006b), Study of spatial and temporal characteristics of L-band scintillations over the Indian low-latitude region and their possible effects on GPS navigation, *Ann. Geophys.*, *24*, 1567–1580, doi:10.5194/angeo-24-1567-2006.

Rastogi, R. G. (1980), Seasonal variation of equatorial spread *F* in the American and Indian zones, *J. Geophys. Res.*, *85*(2), 722–726, doi:10.1029/JA085iA02p00722.

Rastogi, R. G., and J. A. Klobuchar (1990), Ionospheric electron content within the equatorial F_2 layer anomaly belts, *J. Geophys. Res.*, *95*, 19,045–19,052, doi:10.1029/JA095iA11p19045.

Scherliess, L., and B. G. Fejer (1997), Storm time dependence of equatorial disturbance dynamo zonal electric field, *J. Geophys. Res.*, *102*, 24,037–24,046, doi:10.1029/97JA02165.

Singh, S., D. K. Bamgboye, J. P. McClure, and F. S. Johnson (1997), Morphology of equatorial plasma bubbles, *J. Geophys. Res.*, *102*, 20,019–20,029, doi:10.1029/97JA01724.

Sobral, J. H. A., M. A. Abdu, H. Takahashi, M. J. Taylor, E. R. de Paula, C. J. Zamlutti, M. G. de Aquino, and G. L. Borba (2002), Ionospheric plasma bubble climatology over Brazil based on 22 years (1977–1998) of 630 nm airglow observations, *J. Atmos. Sol. Terr. Phys.*, *64*, 1517–1524, doi:10.1016/S1364-6826(02)00089-5.

Sripathi, S., B. Kakad, and A. Bhattacharyya (2011), Study of equinoctial asymmetry in the Equatorial Spread F (ESF) irregularities over Indian region using multi-instrument observations in the descending phase of solar cycle 23, *J. Geophys. Res.*, *116*, A11302, doi:10.1029/2011JA016625.

Stolle, C., H. Lühr, and B. G. Fejer (2008), Relation between the occurrence rate of ESF and the equatorial vertical plasma drift velocity at sunset derived from global observations, *Ann. Geophys.*, *26*, 3979–3988, doi:10.5194/angeo-26-3979-2008.

Su, S.-Y., C. K. Chao, and C. H. Liu (2008), On monthly/seasonal/longitudinal variations of equatorial irregularity occurrences and their relationship with the post-sunset vertical drift velocities, *J. Geophys. Res.*, *113*, A05307, doi:10.1029/2007JA012809.

Takahashi, H., et al. (2009), Simultaneous observation of ionospheric plasma bubbles and mesospheric gravity waves during the SpreadFEx Campaign, *Ann. Geophys.*, *27*(4), 1477–1487, doi:10.5194/angeo-27-1477-2009.

Taori, A., A. K. Patra, and L. M. Joshi (2011), Gravity wave seeding of equatorial plasma bubbles: An investigation with simultaneous *F* region, *E* region, and middle atmospheric measurements, *J. Geophys. Res.*, *116*, A05310, doi:10.1029/2010JA016229.

Tsunoda, R. T. (1985), Control of the seasonal and longitudinal occurrence of equatorial scintillations by the longitudinal gradient in integrated *E*-region Pedersen conductivity, *J. Geophys. Res.*, *90*, 447–456, doi:10.1029/JA090iA01p00447.

Tsunoda, R. T. (2010), On seeding equatorial spread *F* during solstices, *Geophys. Res. Lett.*, *37*, L05102, doi:10.1029/2010GL042576.

Vichare, G., and A. D. Richmond (2005), Simulation studies of the longitudinal variation of evening vertical ionospheric drifts at the magnetic equator during equinox, *J. Geophys. Res.*, *110*, A05304, doi:10.1029/2004JA010720.

Woodman, R. F., and C. LaHoz (1976), Radar observations of *F* region equatorial irregularities, *J. Geophys. Res.*, *81*(31), 5447–5466, doi:10.1029/JA081i031p05447.

Woodman, R. F., J. E. Pingree, and W. E. Swartz (1985), Spread-F-like irregularities observed by the Jicamarca radar during the day-time, *J. Atmos. Terr. Phys.*, *47*(8–10), 867–874.

Yokoyama, T., M. Yamamoto, Y. Otsuka, M. Nishioka, T. Tsugawa, S. Watanabe, and R. F. Pfaff (2011), On post-midnight low-latitude ionospheric irregularities during solar minimum: Equatorial Atmosphere Radar and GPS-TEC observations in Indonesia, *J. Geophys. Res.*, *116*, A11325, doi:10.1029/2011JA016797.

Zhao, B., W. Wan, and L. Liu (2005), Response of equatorial anomaly to the October–November 2003 superstorms, *Ann. Geophys.*, *23*, 693, doi:10.5194/angeo-23-693-2005.